Int. J. Solids Structures Vol. 30, No. 18, pp. 2525–2545, 1993
Printed in Great Britain

0020–7683/93 $6.00+ .00
Pergamon Press Ltd

COMPOSITE CYLINDRICAL SEGMENTS SUBJECTED TO HYGROTHERMAL AND MECHANICAL LOADS

LÁSZLÓ P. KOLLÁR† and JOCELYN M. PATTERSON
Department of Aeronautics and Astronautics, Stanford University, Stanford, California 94305, U.S.A.

(*Received* 28 *August* 1992; *in revised form* 16 *December* 1992)

Abstract—The three-dimensional stress analysis of Kollár and Springer (1992, *Int. J. Solids Structures* **29,** 1499–1517) is applied to a fiber-reinforced organic matrix composite cylindrical segment subjected to hygrothermal and mechanical loads. The segment can have an arbitrary arc length. The straight edges of the segment can be free, fixed or hinged. The wall of the cylindrical segment may be "thin" or "thick". An individual fiber is at the same radial distance from the axis; no other restrictions are placed either on fiber orientations or on stacking sequence. The applied hygrothermal and mechanical loads may vary radially and circumferentially, but not axially. Solutions are presented which yield radially and circumferentially varying strains and stresses inside the composite cylindrical segment. To illustrate the capability of the resulting computer code, sample problems are discussed.

1. INTRODUCTION

In a previous paper (herein referred to as Paper 1) Kollár and Springer (1992) presented a stress analysis applicable to laminated composite cylinders and cylindrical segments. In the present paper we apply the analysis to cylindrical segments and present the equations which are needed, in addition to those in Paper 1, to calculate the displacements, strains and stresses in hygrothermally and mechanically loaded cylindrical segments.

For brevity, the basic equations already given in Paper 1 are not reproduced here. Only those equations are presented which are not in Paper 1 and are needed for the solution of the problem. We do recall from Paper 1, that the solution is based on three-dimensional elasticity equations with the restrictions that the applied loads as well as the strains and stresses may vary in the radial and circumferential directions, but must be independent of the axial direction.

A three-dimensional elasticity solution was employed in the analysis instead of a shell solution, because of our interest in thick cylindrical segments. Shell solutions generally utilize a series approximation perpendicular to the surface. For thick segments these types of solutions may yield inaccurate stress–strain values or require the use of a large number of terms in the series. This makes the solution time consuming. The inaccuracies in the shell become especially significant in the presence of a temperature gradient through the thickness. These shortcomings of shell solutions are overcome by the present three-dimensional analysis.

Detailed literature reviews of shell solutions have been recently presented by Noor and his co-workers (Noor and Burton, 1990; Noor *et al.*, 1991). A review of the three-dimensional elasticity solutions applicable to closed cylinders was given in Paper 1. Analyses pertaining to orthotropic and anisotropic cylindrical segments have been presented by Roy (1991) and Spencer *et al.* (1991), respectively. In both of these analyses the temperature is assumed to be constant, and the stresses and strains are assumed to vary in the radial but not in the circumferential direction. In the present paper the cylindrical segment is anisotropic and the temperature, stresses and strains may vary in the radial as well as in the circumferential directions.

† On leave from the Technical University of Budapest, Department of Reinforced Concrete Structures, 1521 Hungary, Budapest.

2. PROBLEM STATEMENT

We consider a cylindrical segment made of n layers of unidirectional fiber-reinforced composites (Fig. 1). There is no restriction on either the number of plies or the orientation (ply-angle) of the fibers in each ply. Hence the cylindrical segment may be "thick" and the lay-up may be unsymmetric. However, the cylindrical segment must be long, so that the length L is large compared to the thickness h and to the inner r^i and outer r^o radii ($h/L \ll 1$, $r^o/L \ll 1$, $r^i/L \ll 1$).

The cylindrical segment may be either unsupported or supported along the two longitudinal edges. Both edges can be either free, hinged or fixed, or one edge is fixed and the other is hinged, or one edge is fixed and the other is free (Fig. 2).

The cylindrical segment may be subjected to hygrothermal and mechanical loads which may vary in the radial r and circumferential θ directions, but must be independent of the axial coordinate x. Thus, the temperature ΔT and the moisture Δc distribution inside the composite may vary with r and θ but not with x. Here ΔT and Δc are the known temperature and moisture content relative to prescribed reference values T_{ref} and c_{ref}

$$\Delta T(\theta, r) = T - T_{\text{ref}}, \quad \Delta c(\theta, r) = c - c_{\text{ref}}. \tag{1}$$

The cylindrical segment with *unsupported edges* may have edge loads on them as shown in Fig. 3. There may be axial N_x and shear loads Q_1 around the edges. The lengthwise edges may also be subjected to normal loads Q_2 or to distributed moments Q_3. All these loads must be independent of x. In addition, the segment may be subjected to a twisting moment T or a bending moment M. The only restriction is that the loads must be in equilibrium and must not result in rigid body motion.

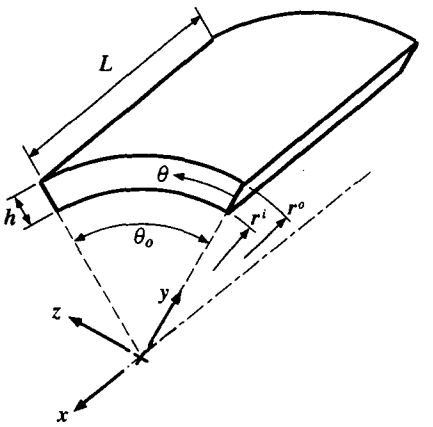

Fig. 1. Geometry of the cylindrical segment.

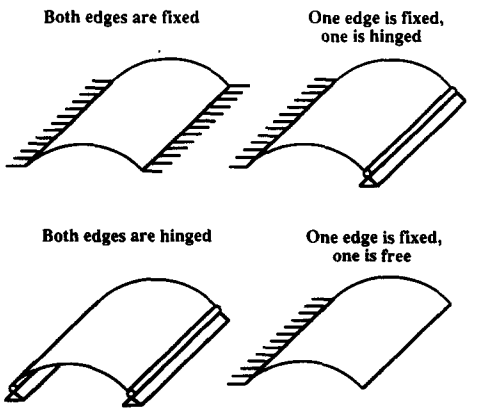

Fig. 2. Conditions along the lengthwise edges of the cylindrical segment.

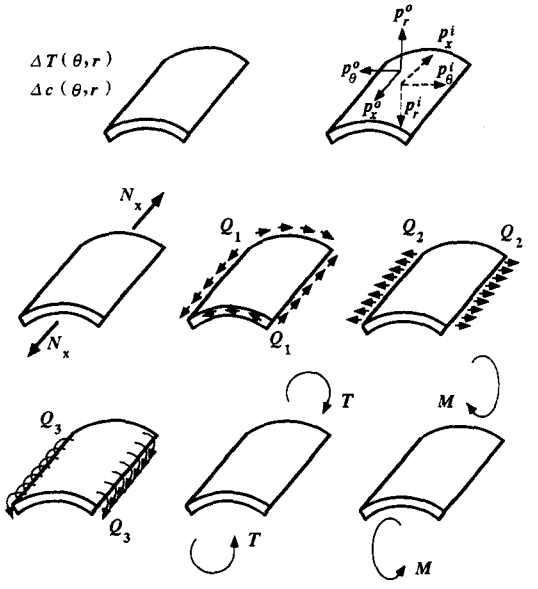

Fig. 3. Loads on the cylindrical segment.

Cylindrical segments *supported along the longitudinal edges* may be subjected to radial, circumferential and axial loads on the inner and outer surfaces. These loads, denoted by p_r^i, p_θ^i, p_x^i; p_r^o, p_θ^o, p_x^o, (Fig. 3), may vary with θ but not with x, and hence must be independent of x.

The objective is to find the stresses and strains inside the composite under the combined temperature, moisture and mechanical loads described above.

3. DISPLACEMENTS

The axial, circumferential and radial displacements in the lth layer have the general form (see Appendix A)

$$\begin{aligned} u^l(x,\theta,r) &= u_o^l(x,\theta,r)+u_F^l(\theta,r)+u_B^l(x,\theta,r),\\ v^l(x,\theta,r) &= v_o^l(x,\theta,r)+v_F^l(\theta,r)+v_B^l(x,\theta,r),\\ w^l(x,\theta,r) &= w_o^l(x,\theta,r)+w_F^l(\theta,r)+w_B^l(x,\theta,r). \end{aligned} \tag{2}$$

The displacements u_o^l, v_o^l, w_o^l are given by eqn (1.9),† u_F^l, v_F^l, w_F^l by eqn (1.15), and u_B^l, v_B^l, w_B^l by eqn (1.46), but, for the reader's convenience, we reproduce these equations in Appendix A. The displacements contain a number of unknown constants in each layer (Table 1), which must be determined from the conditions of no rigid body motion and the boundary conditions. The continuity conditions are given in Tables 1.7–1.10 in Paper 1, and are not reproduced here. The boundary conditions which must be applied in a specific problem are described subsequently.

4. EDGE FORCES AND EDGE DISPLACEMENTS

From the three-dimensional analysis the edge stresses and edge displacements can be determined. For a complete description of the problem, we should specify the stress and/or the displacements at each point on the edges. However it is convenient to prescribe only the stress resultants (edge forces) and/or the displacements of the reference surface. For this purpose we have to define the edge forces and edge displacements.

† The number 1 preceding an equation or table number refers to an equation or table in Paper 1 (Kollár and Springer, 1992).

Table 1. The unknown constants in the displacements, continuity, no rigid body motion, and boundary conditions

	$u_o^\ell, v_o^\ell, w_o^\ell$	$u_F^\ell, v_F^\ell, w_F^\ell$		$u_B^\ell, v_B^\ell, w_B^\ell$
		$j\frac{r}{r_o} \neq 1$	$j\frac{r}{r_o} = 1$	
Unknowns (one layer)	A_1^ℓ, A_2^ℓ $u_a^\ell, u_b^\ell, u_c^\ell, u_d^\ell$ $v_a^\ell, v_b^\ell, v_c^\ell, v_d^\ell$	$G_{jk}^\ell \quad k = 1,2,\ldots,6$ $G_{jk}^{\ell *} \quad j = 1,2,\ldots,$number of Fourier terms		$\kappa^y, H_k^{\ell y}$ $k = 1,2,\ldots,6$ $\kappa^z, H_k^{\ell z}$
Number of unknowns	10*n	(2*6)n for each Fourier term		2+(2*6)n
Continuity conditions	10*(n-1)	(2*6)(n-1) for each Fourier term		(2*6)(n-1)
No rigid body motions	$u_d^1 = 0, v_d^1 = 0$		$G_{j5}^1 = 0, G_{j5}^{1*} = 0$	$H_5^{1y} = 0, H_5^{1z} = 0$
Boundary conditions if no rigid body motions	8	2*6 for each Fourier term	2*5	2*6

Edge forces

At a constant θ cross-section the in-plane and transverse shear forces per unit length are (Fig. 4)

$$t_{\theta x}(\theta) = \int_{r^i}^{r^o} \tau_{x\theta}(\theta, r)\, dr, \tag{3}$$

$$t_{\theta r}(\theta) = \int_{r^i}^{r^o} \tau_{\theta r}(\theta, r)\, dr, \tag{4}$$

where θ and r are the tangential and radial coordinates (Fig. 1). $\tau_{x\theta}$ and $\tau_{\theta r}$ are the shear stresses at the constant θ cross-section, r^i and r^o are the inner and outer radii. The forces due to the hoop stress and the bending and twisting moments (per unit length) are

$$n_\theta(\theta) = \int_{r^i}^{r^o} \sigma_\theta(\theta, r)\, dr, \tag{5}$$

$$m_{\theta x}(\theta) = \int_{r^i}^{r^o} (r - R)\sigma_\theta(\theta, r)\, dr, \tag{6}$$

$$m_{\theta\theta}(\theta) = \int_{r^i}^{r^o} (r - R)\tau_{x\theta}(\theta, r)\, dr, \tag{7}$$

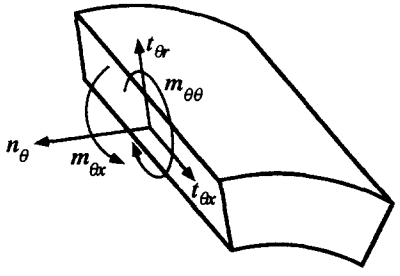

Fig. 4. Edge forces along the lengthwise edges of the cylindrical segment.

where R is the radius of a reference surface which, conveniently, can be taken as the mid-surface of the composite cylindrical segment.

At a constant x cross-section the axial load is

$$N_x = \int_0^{\theta_o} \int_{r^i}^{r^o} r\sigma_x(\theta, r)\, dr\, d\theta. \tag{8}$$

At the same constant x cross-section the torque T and bending moments M_y and M_z are

$$T = \int_0^{\theta_o} \int_{r^i}^{r^o} r^2\tau_{x\theta}(\theta, r)\, dr\, d\theta, \tag{9}$$

$$M_y = \int_0^{\theta_o} \int_{r^i}^{r^o} r^2 \cos\theta\, \sigma_x(\theta, r)\, dr\, d\theta, \tag{10}$$

$$M_z = \int_0^{\theta_o} \int_{r^i}^{r^o} r^2 \sin\theta\, \sigma_x(\theta, r)\, dr\, d\theta, \tag{11}$$

where M_y and M_z are the components of the applied bending moments in the x–y and x–z planes, as shown in Fig. 5. There are also shear forces S_y and S_z at the same constant x cross-section

$$S_y = \int_0^{\theta_o} \int_{r^i}^{r^o} r(\tau_{xr}\cos\theta - \tau_{x\theta}\sin\theta)\, dr\, d\theta, \tag{12}$$

$$S_z = \int_0^{\theta_o} \int_{r^i}^{r^o} r(\tau_{xr}\sin\theta + \tau_{x\theta}\cos\theta)\, dr\, d\theta. \tag{13}$$

The forces acting along the curved edges (N_x, T, M_y, M_z, S_y and S_z) are denoted by Ω_1, Ω_2,

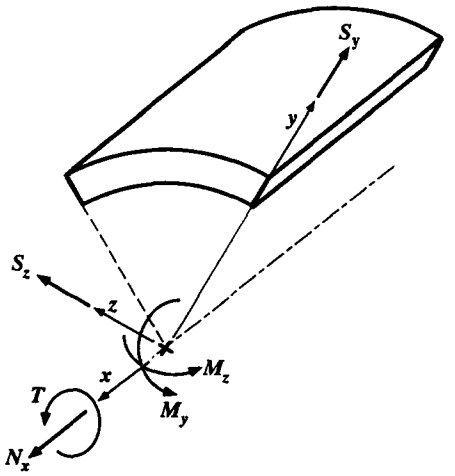

Fig. 5. Edge forces along the curved edges of the cylindrical segment.

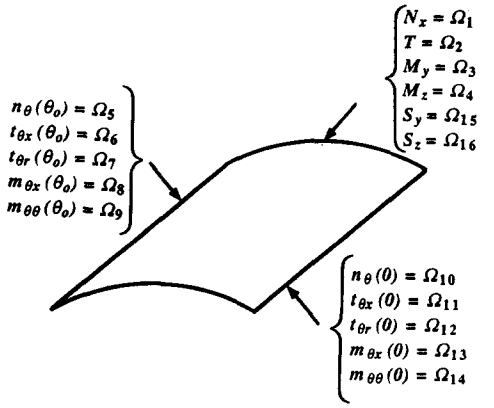

Fig. 6. Definition of the 16 edge forces.

Ω_3, Ω_4, Ω_{15}, Ω_{16} (Fig. 6). On each straight edge there are five forces: n_θ, $t_{\theta x}$, $t_{\theta r}$, $m_{\theta x}$, $m_{\theta\theta}$, and these are denoted by Ω_5, Ω_6, Ω_7, Ω_8, Ω_9 on the $\theta = \theta_o$ edge, and by Ω_{10}, Ω_{11}, Ω_{12}, Ω_{13}, Ω_{14} on the $\theta = 0$ edge (Fig. 6).

The 16 edge forces (Ω_1–Ω_{16}) must satisfy the six equilibrium equations for the cylindrical segment. In the absence of surface forces, the force equilibrium in the x, y and z directions are

$$\begin{aligned} \Omega_6 - \Omega_{11} &= 0, \\ \Omega_7 \cos\theta_o - \Omega_5 \sin\theta_o - \Omega_{12} &= 0, \\ \Omega_7 \sin\theta_o + \Omega_5 \cos\theta_o - \Omega_{10} &= 0, \end{aligned} \tag{14}$$

and the moment equilibriums about the x, y and z axes are

$$\begin{aligned} \Omega_8 - \Omega_{13} + (\Omega_5 - \Omega_{10})R &= 0, \\ \Omega_9 \cos\theta_o - \Omega_{14} - S_y &= 0, \\ \Omega_9 \sin\theta_o - S_z &= 0. \end{aligned} \tag{15}$$

Taking into account these six conditions, only 10 of the 16 edge forces can be chosen independently.

On the inner and outer surfaces, radial (r), circumferential (θ), and axial (x) surface loads can be prescribed: $p_r^i, p_\theta^i, p_x^i, p_r^o, p_\theta^o, p_x^o$. These loads must be equal to the corresponding surface stresses:

- on the inner surface ($r = r^i$)

$$p_r^i = \sigma_r^1(\theta, r^i), \quad p_\theta^i = \tau_{r\theta}^1(\theta, r^i), \quad p_x^i = \tau_{rx}^1(\theta, r^i), \tag{16}$$

- on the outer surface ($r = r^o$)

$$p_r^o = \sigma_r^n(\theta, r^o), \quad p_\theta^o = \tau_{r\theta}^n(\theta, r^o), \quad p_x^o = \tau_{rx}^n(\theta, r^o), \tag{17}$$

where p is the force per unit area. If the displacements are given by a Fourier series (Appendix A), we must also express the loads in the form of a Fourier series (Appendix B).

Edge displacements

The edges of the cylindrical segments may move relative to each other resulting in 10 different possible relative displacements. These we denote as the edge displacements

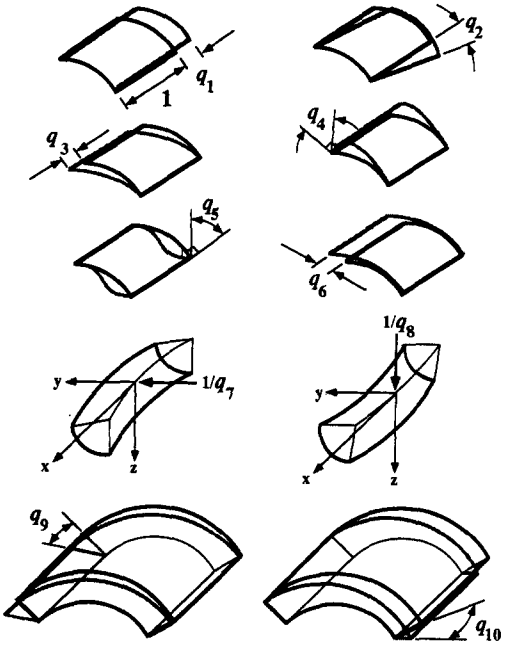

Fig. 7. Definition of the 10 edge displacements.

$q_1, q_2, \ldots, q_{10}$ (Fig. 7). Table 2 shows these displacements expressed in terms of the axial u, circumferential v, and radial w displacements of the edges.

The edge rotations q_4 and q_5 are defined in terms of the angular rotations of the left edge, ϕ_R, the right edge, ϕ_L, and the rigid body rotation, ϕ_B (Fig. 8)

$$\varphi_L = \frac{1}{h}[v(0, \theta_o, r^o) - v(0, \theta_o, r^i)]_{\kappa^y = \kappa^z = 0}, \tag{18}$$

$$\varphi_R = \frac{1}{h}[v(0, 0, r^o) - v(0, 0, r^i)]_{\kappa^y = \kappa^z = 0}, \tag{19}$$

$$\varphi_B = \frac{1}{2R \sin\frac{\theta_o}{2}}\left[(w(0,0,R) - w(0,\theta_o,R))\cos\frac{\theta_o}{2} + (v(0,0,R) + v(0,\theta_o,R))\sin\frac{\theta_o}{2}\right]_{\kappa^y = \kappa^z = 0}. \tag{20}$$

5. EDGE LOADS ONLY—FREE EDGES

First we consider a cylindrical segment which is subjected to the edge loads shown in Fig. 3, but to no hygrothermal loads and no surface loads. Cylindrical segments subjected to the latter type of loads are discussed subsequently.

The solution is assembled from the individual solutions of the following 10 cases:

(1) Axially loaded cylindrical segment with the axis remaining straight (Table 3).
(2) Cylindrical segment subjected to torque with the axis remaining straight (Table 3).
(3) Cylindrical segment subjected to shear force with the axis remaining straight (Table 3).
(4) Cylindrical segment subjected to distributed bending moments along the straight edges with axis remaining straight (Table 3).
(5) Cylindrical segment under curvature in the x–y plane (Table 4).
(6) Cylindrical segment under curvature in the x–z plane (Table 4).

Table 2. Description of edge displacements

Axial displacement of the curved boundaries	$q_1 = \frac{\partial u(z,\theta,R)}{\partial z}\Big\|_{\kappa^y=\kappa^z=0}$	(21)
Rotation of the straight boundaries	$q_2 = \frac{\partial v(z,\theta,R)}{\partial z}\Big\|_{\kappa^y=\kappa^z=0}$	(22)
Axial displacement of one of the straight edges relative to the other one	$q_3 = u(0,\theta_o,R) - u(0,0,R)\Big\|_{\kappa^y=\kappa^z=0}$	(23)
Rotation of left straight boundary with respect to the plane lying on the two straight edges	$q_4 = \varphi_L - \varphi_B$	(24)
Rotation of right straight boundary with respect to the plane lying on the two straight edges	$q_5 = \varphi_R - \varphi_B$	(25)
Relative edge displacement between the two straight edges	$q_6 = \left[(w(0,\theta_o,R) + w(0,0,R))\sin\frac{\theta_o}{2} + (v(0,\theta_o,R) - v(0,0,R))\cos\frac{\theta_o}{2}\right]_{\kappa^y=\kappa^z=0}$	(26)
Curvature of the cylindrical segment's axis in the $x-y$ plane	$q_7 = \kappa^y$	(27)
Curvature of the cylindrical segment's axis in the $x-z$ plane	$q_8 = \kappa^z$	(28)
Angular deformation of the left straight edge	$q_9 = \frac{1}{h}\left[u(0,\theta_o,r^o) - v(0,\theta_o,r^i)\right]_{\kappa^y=\kappa^z=0}$	(29)
Angular deformation of the right straight edge	$q_{10} = \frac{1}{h}\left[u(0,0,r^o) - u(0,0,r^i)\right]_{\kappa^y=\kappa^z=0}$	(30)

(7) Cylindrical segment subjected to distributed horizontal forces along the straight edges with the axis remaining straight (Table 5).
(8) Cylindrical segment subjected to distributed vertical forces and distributed bending moments along the straight edges with the axis remaining straight (Table 6).

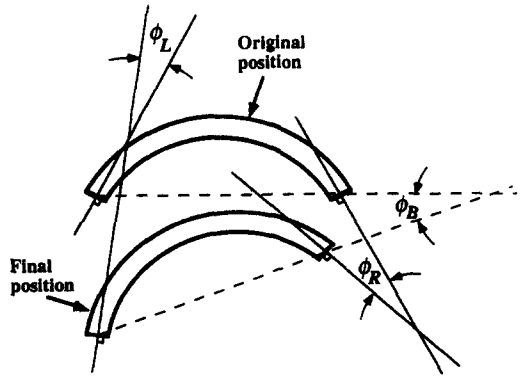

Fig. 8. Explanation of edge rotation.

Table 3. Loads and displacements in the first to fourth cases

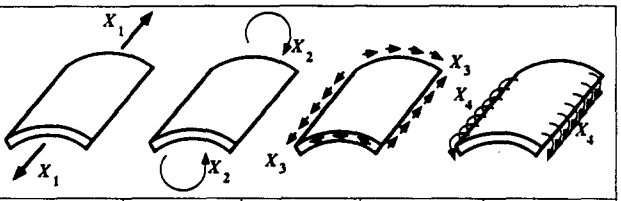

	Case 1	Case 2	Case 3	Case 4
surface loads and	$p_r^i = p_\theta^i = p_x^i = p_r^o = p_\theta^o = p_x^o = 0$			
prescribed edge loads	$N_x = X_1$	$N_x = 0$	$N_x = 0$	$N_x = 0$
	$T = 0$	$T = X_2$	$T = 0$	$T = 0$
	$t_{\theta x} = 0$	$t_{\theta x} = 0$	$t_{\theta x} = X_3$	$t_{\theta x} = 0$
	$m_{\theta x} = 0$	$m_{\theta x} = 0$	$m_{\theta x} = 0$	$m_{\theta x} = X_4$
displacements u	u_o^ℓ			
(Eq.A2) v	v_o^ℓ			
w	w_o^ℓ			
number of unknowns	8			
conditions to	$\sigma_{ro}^1(r^i) = \tau_{r\theta o}^1(r^i) = \tau_{rxo}^1(r^i) = \sigma_{ro}^n(r^o) = 0$			
determine the constants	$N_x = X_1$	$N_x = 0$	$N_x = 0$	$N_x = 0$
(Table B1)	$T = 0$	$T = X_2$	$T = 0$	$T = 0$
	$t_{\theta x} = 0$	$t_{\theta x} = 0$	$t_{\theta x} = X_3$	$t_{\theta x} = 0$
	$m_{\theta x} = 0$	$m_{\theta x} = 0$	$m_{\theta x} = 0$	$m_{\theta x} = X_4$

Table 4. Loads and displacements in the fifth and sixth cases

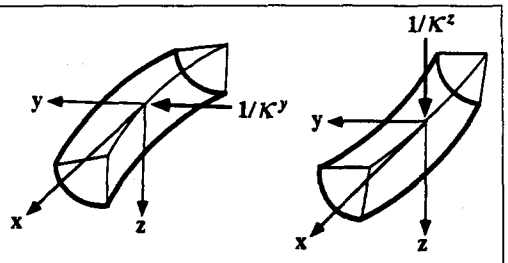

	Case 5	Case 6
surface load and	$p_r^i = p_\theta^i = p_x^i = p_r^o = p_\theta^o = p_x^o = 0$	
prescribed edge loads		
displacements u	u_B^ℓ	
(Eq.A4) v	v_B^ℓ	
w	w_B^ℓ	
number of unknowns	12	
conditions to	$\kappa^y = X_5 \quad \kappa^z = 0$	$\kappa^y = 0 \quad \kappa^z = X_6$
determine the	$\hat{\sigma}_{rB}^{1y}(r^i) = \hat{\tau}_{r\theta B}^{1y}(r^i) = \hat{\tau}_{rxB}^{1y}(r^i) = 0$	
unknowns	$\hat{\sigma}_{rB}^{1z}(r^i) = \hat{\tau}_{r\theta B}^{1z}(r^i) = \hat{\tau}_{rxB}^{1z}(r^i) = 0$	
(Table B1)	$\hat{\sigma}_{rB}^{ny}(r^o) = \hat{\sigma}_{rB}^{nz}(r^o) = \hat{\tau}_{rxB}^{ny}(r^o) = \hat{\tau}_{rxB}^{nz}(r^o) = 0$	

Table 5. Loads and displacements in the seventh case

Case 7

	Case 7 (=)	Case 7a	Case 7b (+)
surface loads and	$p_\theta^i = p_x^i = p_r^o = p_\theta^o = p_x^o = 0$		
prescribed edge loads	$p_r^i = 0$	$p_r^i = X_7 \sin 3\frac{\pi}{\theta_o}\theta$	$p_r^i = -X_7 \sin 3\frac{\pi}{\theta_o}\theta =$ $= \sum_{j=0,2,4,\ldots} \hat{p}_{rj}^i \cos j\frac{\pi}{\theta_o}\theta$ $N_x = 0 \quad T = 0$ $t_{\theta x} = 0 \quad m_{\theta x} = 0$
displacements u (Eq.A1 – A3)		$-u_3^{\ell *} \cos 3\frac{\pi}{\theta_o}\theta$	$u_o^\ell + \sum_{j=2,4,\ldots} u_j^\ell \sin j\frac{\pi}{\theta_o}\theta$
v		$-v_3^{\ell *} \cos 3\frac{\pi}{\theta_o}\theta$	$v_o^\ell + \sum_{j=2,4,\ldots} v_j^\ell \sin j\frac{\pi}{\theta_o}\theta$
w		$w_3^{\ell *} \sin 3\frac{\pi}{\theta_o}\theta$	$w_o^\ell + \sum_{j=2,4,\ldots} w_j^\ell \cos j\frac{\pi}{\theta_o}\theta$
number of unknowns		6	8 for the zeroth term 6 for the other terms
conditions to determine the unknowns (Table B1)		$\hat{\sigma}_{r3}^{1*}(r^i) = X_7$ $\hat{\sigma}_{r3}^{n*}(r^o) = 0$ $\hat{\tau}_{r\theta 3}^{1*}(r^i) = 0$ $\hat{\tau}_{r\theta 3}^{n*}(r^o) = 0$ $\hat{\tau}_{rz3}^{1*}(r^i) = 0$ $\hat{\tau}_{rz3}^{n*}(r^o) = 0$	$N_x = 0 \quad T = 0$ $t_{\theta x} = 0 \quad m_{\theta x} = 0$ $\sigma_{ro}^1(r^i) = \hat{p}_{ro}^i \quad \tau_{r\theta o}^1(r^i) = 0$ $\tau_{rzo}^1(r^i) = 0 \quad \sigma_{ro}^n(r^o) = 0$ $\hat{\sigma}_{rj}^1(r^i) = \hat{p}_{rj}^i \quad \hat{\sigma}_{rj}^n(r^o) = 0$ $\hat{\tau}_{r\theta j}^1(r^i) = 0 \quad \hat{\tau}_{r\theta j}^n(r^o) = 0$ $\hat{\tau}_{rzj}^1(r^i) = 0 \quad \hat{\tau}_{rzj}^n(r^o) = 0$ $j = 2, 4, \ldots$

Remark $$\hat{p}_{rj}^i = \begin{cases} -X_7 \frac{2}{3\pi} & \text{if } j = 0 \\ X_7 \frac{12}{(j^2-9)\pi} & \text{if } j \geq 2 \end{cases}$$

(9) Cylindrical segment subjected to an anticlockwise distributed twisting moment along the right edge and to a clockwise distributed twisting moment along the left edge with the axis remaining straight (Table 7).
(10) Cylindrical segment subjected to clockwise distributed twisting moments along both edges with the axis remaining straight (Table 8).

First we present the boundary conditions corresponding to each of these problems. We then show how to assemble the individual solutions to provide a solution for the general problem depicted in Fig. 3.

Cases (1)–(4)

Consider a cylindrical segment on which there are no surface loads. In Case (1) an axial load $N_x = X_1$ is applied while the applied torque T, shear force $t_{\theta x}$ and bending moment $m_{\theta x}$ are zero. In Case (2) a torque $T = X_2$, in Case (3) a shear force $t_{\theta x} = X_3$, and in Case (4) a bending moment $m_{\theta x} = X_4$ is applied while the other three edge forces are zero. In each case [Cases (1)–(4)] the axis of the cylinder remains straight. The displacements which satisfy these conditions are given in Table 3. These displacements contain eight unknown constants, which can be determined with the conditions given in Table 3.

Cases (5)–(6)

Consider a cylindrical segment on which there are no surface loads. In Case (5) the cylindrical segment's axis has a curvature in the x–y plane ($\kappa^y = X_5$), and the curvature in

Table 6. Loads and displacements in the eighth case

Case 8

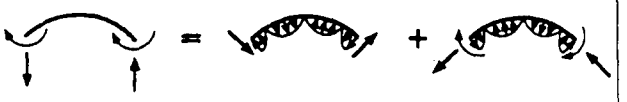

	Case 8 (≡)	Case 8a	(+) Case 8b
surface loads and prescribed edge loads	$p_\theta^i = p_z^i = p_r^o = p_\theta^o = p_z^o = 0$		
	$p_r^i = 0$	$p_r^i = X_8 \cos 3\frac{\pi}{\theta_o}\theta$ $= \sum_{j=2,4,\ldots} \hat{p}_{rj}^{i*} \sin j\frac{\pi}{\theta_o}\theta$	$p_r^i = -X_8 \cos 3\frac{\pi}{\theta_o}\theta$
displacements u (Eq.A1 – A3)		$-\sum_{j=2,4,\ldots} u_j^{\ell *} \cos j\frac{\pi}{\theta_o}\theta$	$u_3^\ell \sin 3\frac{\pi}{\theta_o}\theta$
v		$-\sum_{j=2,4,\ldots} v_j^{\ell *} \cos j\frac{\pi}{\theta_o}\theta$	$v_3^\ell \sin 3\frac{\pi}{\theta_o}\theta$
w		$\sum_{j=2,4,\ldots} w_j^{\ell *} \sin j\frac{\pi}{\theta_o}\theta$	$w_3^\ell \cos 3\frac{\pi}{\theta_o}\theta$
number of unknowns		6 for each Fourier term	6
conditions to determine the unknowns (Table B1)		$\hat{\sigma}_{rj}^{1*}(r^i) = \hat{p}_{rj}^{i*}$ $\hat{\sigma}_{rj}^{n*}(r^o) = 0$ $\hat{\tau}_{r\theta j}^{1*}(r^i) = 0$ $\hat{\tau}_{r\theta j}^{n*}(r^o) = 0$ $\hat{\tau}_{rzj}^{1*}(r^i) = 0$ $\hat{\tau}_{rzj}^{n*}(r^o) = 0$ $j = 2, 4, \ldots$	$\hat{\sigma}_{r3}^1(r^i) = -X_8$ $\hat{\sigma}_{r3}^n(r^o) = 0$ $\hat{\tau}_{r\theta 3}^1(r^i) = 0$ $\hat{\tau}_{r\theta 3}^n(r^o) = 0$ $\hat{\tau}_{rz3}^1(r^i) = 0$ $\hat{\tau}_{rz3}^n(r^o) = 0$

Remark $\hat{p}_{rj}^{i*} = -X_8 \frac{4j}{(j-3)(j+3)\pi}$

the x–z plane is zero ($\kappa^z = 0$). In Case (6) the curvature in the x–y plane is zero ($\kappa^y = 0$) and in the x–z plane is not zero ($\kappa^z = X_6$). The displacements which satisfy these conditions are given in Table 4. These displacements contain 12 unknown constants, which can be determined with the conditions given in Table 4.

Cases (7)–(10)

In the Cases (7)–(10) the axis of the segment remains straight. We place different prescribed loads on the (inner) surface of the cylindrical segment. In Cases (7a, b) and (8a, b) compressive radial forces are applied, while in Cases (9a, b) and (10a, b) tangential forces are applied in the manner illustrated in Tables 5–8. In each case [Cases (7)–(10)] the sum (Case "a" plus Case "b") of the surface forces is zero. The displacements corresponding to each of these cases are given in Tables 5–8. The conditions required to determine the unknowns in the displacements are also given in these tables.

For each case [Cases (7)–(10)] the surface loads are zero. However, the solutions obtained for each of these cases are different, because the edge loads are different.

Combined loading

Cases (1)–(10) provide the boundary conditions for a cylindrical segment subjected to specific loads. The 16 edge forces have been denoted previously by $\Omega_j (j = 1, 2, \ldots, 16)$. [See eqns (3)–(13)]. The edge forces resulting from Cases (1)–(10) are denoted by Ω_{ij} where i takes the values from 1 through 10 due to the 10 cases. Solutions to the 10 problems provide the edge forces Ω_{ij} in terms of 10 constants X_1–X_{10}. To complete the solution it is required to find these remaining 10 constants. X_j appears as a multiplier in each Ω_{ij} term and hence can be factored out. Thus it is convenient to introduce the parameter

Table 7. Loads and displacements in the ninth case

Case 9 			
	Case 9 (=)	Case 9a (+)	Case 9b
surface loads and	$p_r^i = p_\theta^i = p_r^o = p_\theta^o = p_x^o = 0$		
prescribed edge loads	$p_x^i = 0$	$p_x^i = X_9 \sin 2\frac{\pi}{\theta_o}\theta$	$p_x^i = -X_9 \sin 2\frac{\pi}{\theta_o}\theta = \sum_{j=1,3,\ldots} \hat{p}_{xj}^{i*} \cos j\frac{\pi}{\theta_o}\theta$
displacements u		$u_2^\ell \sin 2\frac{\pi}{\theta_o}\theta$	$-\sum_{j=1,3,\ldots} u_j^{\ell *} \cos j\frac{\pi}{\theta_o}\theta$
(Eq.A1 – A3) v		$v_2^\ell \sin 2\frac{\pi}{\theta_o}\theta$	$-\sum_{j=1,3,\ldots} v_j^{\ell *} \cos j\frac{\pi}{\theta_o}\theta$
w		$w_2^\ell \cos 2\frac{\pi}{\theta_o}\theta$	$\sum_{j=1,3,\ldots} w_j^{\ell *} \sin j\frac{\pi}{\theta_o}\theta$
number of unknowns		6	6 for each Fourier term
conditions to determine the unknowns (Table B1)		$\hat{\sigma}_{r2}^1(r^i) = 0$ $\hat{\sigma}_{r2}^n(r^o) = 0$ $\hat{\tau}_{r\theta 2}^1(r^i) = 0$ $\hat{\tau}_{r\theta 2}^n(r^o) = 0$ $\hat{\tau}_{rx2}^1(r^i) = X_9$ $\hat{\tau}_{rx2}^n(r^o) = 0$	$\hat{\sigma}_{rj}^{1*}(r^i) = 0$ $\hat{\sigma}_{rj}^{n*}(r^o) = 0$ $\hat{\tau}_{r\theta j}^{1*}(r^i) = 0$ $\hat{\tau}_{r\theta j}^{n*}(r^o) = 0$ $\hat{\tau}_{rxj}^{1*}(r^i) = \hat{p}_{xj}^{i*}$ $\hat{\tau}_{rxj}^{n*}(r^o) = 0$ $j = 1, 3, \ldots$

Remark $\hat{p}_{xj}^{i*} = X_9 \dfrac{8}{\pi(j-2)(j+2)}$

$$\omega_{ij} = \frac{\Omega_{ij}}{X_j}. \tag{31}$$

On each edge the total force Ω_i is the sum of the edge forces given by Cases (1)–(10). These total edge forces are

$$\Omega_i = \sum_{j=1}^{10} \Omega_{ij} = \sum_{j=1}^{10} \omega_{ij} X_j. \tag{32}$$

From Table 9 and eqn (32) we have

$$\begin{bmatrix} \omega_{11} & \omega_{12} & \ldots & \omega_{110} \\ \omega_{21} & \ldots & \ldots & \ldots \\ \omega_{31} & \ldots & \ldots & \ldots \\ \omega_{41} & \ldots & \ldots & \ldots \\ \omega_{51} & \ldots & \ldots & \ldots \\ \omega_{61} & \ldots & \ldots & \ldots \\ \omega_{71} & \ldots & \ldots & \ldots \\ \omega_{81} & \ldots & \ldots & \ldots \\ \omega_{91} & \ldots & \ldots & \ldots \\ \omega_{141} & \ldots & \ldots & \omega_{1410} \end{bmatrix} \begin{bmatrix} X_1 \\ X_2 \\ X_3 \\ X_4 \\ X_5 \\ X_6 \\ X_7 \\ X_8 \\ X_9 \\ X_{10} \end{bmatrix} = \begin{bmatrix} N_x \\ T \\ M_y \\ M_z \\ Q_2 \cos(\theta_o/2) \\ Q_1 \\ Q_2 \sin(\theta_o/2) \\ Q_3 \\ 0 \\ 0 \end{bmatrix}, \tag{33}$$

where N_x, T and Q_1–Q_3 are the applied loads (see Fig. 3), and M_y and M_z are the y and z components of the applied bending moment M (Fig. 5).

Table 8. Loads and displacements in the tenth case

	Case 10 (=)	Case 10a	Case 10b (+)
surface loads and prescribed edge loads	$p_r^i = p_\theta^i = p_r^o = p_\theta^o = p_z^o = 0$		
	$p_z^i = 0$	$p_z^i = X_{10}\cos 2\frac{\pi}{\theta_o}\theta = \sum_{j=1,3,\ldots} \hat{p}_{zj}^i \sin j\frac{\pi}{\theta_o}\theta$	$p_z^i = -X_{10}\cos 2\frac{\pi}{\theta_o}\theta$
displacements u (Eq.A1 – A3)		$\sum_{j=1,3,\ldots} u_j^\ell \sin j\frac{\pi}{\theta_o}\theta$	$-u_2^{\ell *}\cos 2\frac{\pi}{\theta_o}\theta$
v		$\sum_{j=1,3,\ldots} v_j^\ell \sin j\frac{\pi}{\theta_o}\theta$	$-v_2^{\ell *}\cos 2\frac{\pi}{\theta_o}\theta$
w		$\sum_{j=1,3,\ldots} w_j^\ell \cos j\frac{\pi}{\theta_o}\theta$	$w_2^{\ell *}\sin 2\frac{\pi}{\theta_o}\theta$
number of unknowns		6 for each Fourier term	6
conditions to determine the unknowns (Table B1)		$\hat{\sigma}_{rj}^1(r^i) = 0$ $\hat{\sigma}_{rj}^n(r^o) = 0$ $\hat{\tau}_{r\theta j}^1(r^i) = 0$ $\hat{\tau}_{r\theta j}^n(r^o) = 0$ $\hat{\tau}_{rzj}^1(r^i) = \hat{p}_{zj}^i$ $\hat{\tau}_{rzj}^n(r^o) = 0$ $j = 1, 3, \ldots$	$\hat{\sigma}_{r2}^{1*}(r^i) = 0$ $\hat{\sigma}_{r2}^{n*}(r^o) = 0$ $\hat{\tau}_{r\theta 2}^{1*}(r^i) = 0$ $\hat{\tau}_{r\theta 2}^{n*}(r^o) = 0$ $\hat{\tau}_{rz2}^{1*}(r^i) = -X_{10}$ $\hat{\tau}_{rz2}^{n*}(r^o) = 0$

Remark $\quad \hat{p}_{zj}^i = -X_{10}\dfrac{4j}{\pi(j-2)(j+2)}$

Table 9. Edge forces due to loads N_x, T, M_y and M_z (components of M), Q_1, Q_2 and Q_3

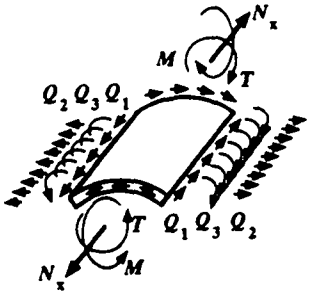

$\Omega_1 = N_x$
$\Omega_2 = T$
$\Omega_3 = M_y$
$\Omega_4 = M_z$
$\Omega_5 = Q_2 \cos \frac{\theta_x}{2}$
$\Omega_6 = Q_1$
$\Omega_7 = Q_2 \sin \frac{\theta_x}{2}$
$\Omega_8 = Q_3$
$\Omega_9 = 0$
$\Omega_{14} = 0$

Table 10. Displacements, edge displacements, and edge forces for solution of cylindrical segment in terms of the ten load cases

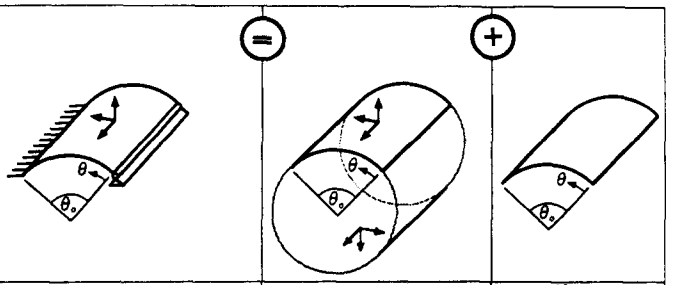

Displacements	u^{ℓ}	u^{ℓ}_{CL}	$\sum_{j=1}^{10} u^{\ell}_{j}$
	v^{ℓ}	v^{ℓ}_{CL}	$\sum_{j=1}^{10} v^{\ell}_{j}$
	w^{ℓ}	w^{ℓ}_{CL}	$\sum_{j=1}^{10} w^{\ell}_{j}$
Relative displ. of "upper" part ($i = 1,2,...12$)	q_i	q_{iCL}	$\sum_{j=1}^{10} q_{ij}$
Forces of the "upper" part	Ω_i	Ω_{iCL}	$\sum_{j=1}^{10} \Omega_{ij}$

From eqn (33) the 10 unknowns X_1–X_{10} can be calculated. Once X_1–X_{10} are known, the displacements for each of the 10 cases can be calculated. These displacements are represented by u^l_s, v^l_s, w^l_s, where s equals $1,2,\ldots,10$. Once the displacements for each individual case are known, the displacements of the cylindrical segment under the action of the combined loading are given by

$$u^l_{\text{total}} = \sum_{s=1}^{10} u^l_s, \quad v^l_{\text{total}} = \sum_{s=1}^{10} v^l_s, \quad w^l_{\text{total}} = \sum_{s=1}^{10} w^l_s. \tag{34}$$

6. SURFACE AND TEMPERATURE LOADS

Both straight edges of the cylindrical segment may be hinged or fixed, or one of the edges is fixed while the other one is either hinged or free (Fig. 2). The segment is subjected to temperature ΔT and moisture Δc load and to radial p_r, circumferential p_θ, and axial p_x surface loads on the inner and outer surface (Fig. 3). Additionally, if there are only temperature and moisture induced loads, both straight edges of the cylindrical segment may be free. The calculation proceeds along the following steps (Table 10).

Step 1. We consider the cylindrical segment with the imposed temperature, moisture and surface loads.
Step 2. We extend the actual cylindrical segment forming an imaginary closed cylinder. We impose temperature, moisture and surface loads on the imaginary part in such a way that the entire closed cylinder remains in equilibrium and does not undergo rigid body motion.
Step 3. Under the imposed load (see Step 2), we calculate the forces, moments and displacements, strains and stresses in the closed cylinder by the procedure described in detail in Kollár *et al.* (1992) for closed cylinders. The displacements calculated in this manner are designated as $u^l_{\text{CL}}, v^l_{\text{CL}}$ and w^l_{CL}.
Step 4. The displacements calculated in Step 3 are added to the total displacements of the segment calculated previously for Cases (1)–(10). The result is

Table 11. Boundary conditions for a cylindrical segment with (a) both edges fixed, (b) the left edge fixed and the right edge hinged, (c) both edges hinged, (d) the left edge fixed and the right edge free, (e) both edges free

	a)	b)	c)	d)	e)
	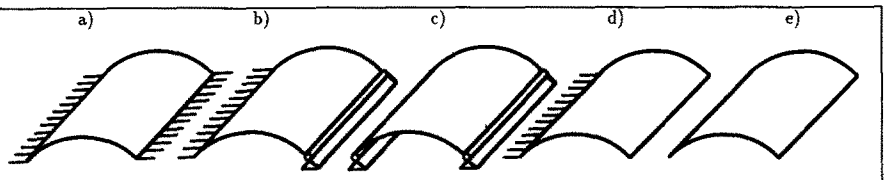				
Prescribed edge forces		$\Omega_{13} = 0$	$\Omega_8 = 0$ $\Omega_{13} = 0$	$\Omega_{10} = 0$ $\Omega_{11} = 0$ $\Omega_{12} = 0$ $\Omega_{13} = 0$ $\Omega_{14} = 0$	$\Omega_1 = 0$ $\Omega_2 = 0$ $\Omega_3 = 0$ $\Omega_4 = 0$ $\Omega_5 = 0$ $\Omega_6 = 0$ $\Omega_7 = 0$ $\Omega_8 = 0$ $\Omega_9 = 0$ $\Omega_{14} = 0$
Prescribed edge displacements	$q_1 = 0$ $q_2 = 0$ $q_3 = 0$ $q_4 = 0$ $q_5 = 0$ $q_6 = 0$ $q_7 = 0$ $q_8 = 0$ $q_9 = 0$ $q_{10} = 0$	$q_1 = 0$ $q_2 = 0$ $q_3 = 0$ $q_4 = 0$ $q_6 = 0$ $q_7 = 0$ $q_8 = 0$ $q_9 = 0$ $q_{10} = 0$	$q_1 = 0$ $q_2 = 0$ $q_3 = 0$ $q_6 = 0$ $q_7 = 0$ $q_8 = 0$ $q_9 = 0$ $q_{10} = 0$	$q_1 = 0$ $q_2 = 0$ $q_7 = 0$ $q_8 = 0$ $q_9 = 0$	

$$u^l_{SEG} = u^l_{CL} + u^l_{total}, \quad v^l_{SEG} = v^l_{CL} + v^l_{total}, \quad w^l_{SEG} = w^l_{CL} + w^l_{total}, \tag{35}$$

where u^l_{total}, v^l_{total}, w^l_{total} are defined by eqn (34).

The three displacements in eqn (35) contain the 10 unknowns $X_1, X_2, \ldots, X_{10}$. These must be obtained from the appropriate 10 boundary conditions.

(A) When both edges are fixed the boundary conditions require that the displacements of each edge are zero. These conditions are listed in Table 11. By substituting the displacements [eqns (35)] into the expression for $q_1, q_2, \ldots, q_{10}$ [eqns (21)–(30)] 10 equations are obtained from which the 10 unknown X values can be calculated.

(B) When one edge is fixed and one is hinged, the boundary conditions require that the displacements along the fixed edge are zero, and along the hinged edge can undergo only rotation. In addition, the moment about the hinged edge must be zero. The corresponding 10 boundary conditions are listed in Table 11. The edge displacements are calculated as in point A. The edge force Ω_{13} is calculated by substituting the displacements into eqn (6). The 10 conditions in Table 11 yield the required 10 X values.

(C) When both straight edges are hinged, these edges can undergo only rotation, and there can be no moments about these edges ($\Omega_8 = \Omega_{13} = 0$). The corresponding 10 boundary conditions needed to be calculated are given in Table 11.

(D) When one straight edge is free and one is fixed, the boundary conditions require that the displacements of the fixed edge are zero, and all the edge forces along the free edge are zero. The corresponding 10 boundary conditions needed for solving X_1–X_{10} are given in Table 11. Note that q_4 (the rotation of the left straight edge) is not zero: the segment can undergo rigid body rotation.

(E) Both edges may be free when only temperature and moisture induced loads are present. In this problem the boundary condition is required that all the edge forces are zero. The 10 expressions representing the 10 boundary conditions needed to calculate X_1–X_{10} are listed in Table 11.

7. METHOD OF SOLUTION

The equations presented in Paper 1 together with those given in the present paper form a complete set for calculating the displacements, stresses and strains under specified boundary conditions. Solution of these equations requires extensive analytical and numerical calculations.

Table 12. Input and output parameters in the SEGMENT computer code

INPUTS

Geometry
- -arc length, θ_o
- -inner radius, r^i
- -thickness of one ply, h_o
- -number of ply groups, n
  - -number of plies in each ply group, m_i
  - -direction (angle) of fibers in each ply group, φ_i

Boundary Conditions
- -Both straight edges are fixed
- -Left edge is fixed; right edge is hinged
- -Both straight edges are hinged
- -Left edge is fixed; right edge is free
- -Both straight edges are free

Material (on-axis) properties
- -Longitudinal Young's modulus, E_1
- -Transverse in-plane Young's modulus, E_2
- -Transverse out-of-plane Young's modulus, E_3
- -Shear moduli, G_{23}, G_{31}, G_{12}
- -Poisson's ratios, $\nu_{23}, \nu_{31}, \nu_{12}$
- -Longitudinal thermal expansion coefficient, α_1
- -Transverse in-plane thermal expansion coefficient, α_2
- -Transverse out-of-plane thermal expansion coefficient, α_3

Loads
- -Edge forces on the curved boundaries
  - -Tensile force, N_x
  - -Torque, T
  - -Bending moment in the $x-y$ plane, M_y
  - -Bending moment in the $y-z$ plane, M_x
- -Edge forces on the straight lengthwise boundaries
  - -Shear force, Q_1
  - -Normal force, Q_2
  - -Distributed moment, Q_3
- -Surface loads on the inner surface, p_r^i, p_θ^i, p_z^i
- -Surface loads on the outer surface, p_r^o, p_θ^o, p_z^o
- -Change in temperature, ΔT

OUTPUTS
- -Stresses in each ply, $\sigma_x, \sigma_\theta, \sigma_r, \tau_{\theta r}, \tau_{xr}, \tau_{\theta x}$
- -Displacements at the inner and outer surfaces, u, v, w

The analytical calculations were performed with a symbolic manipulator, "Mathematica" (Wolfram, 1991). A computer code (designated as SEGMENT) was written for performing the calculations. In the developed Fortran program, we used the following available packages: EISPACK (Smith *et al.*, 1976), LINPACK (Dongarra *et al.*, 1978) and Numerical Recipes (Press *et al.*, 1986). The input parameters required for and the output parameters provided by the code are given in Table 12.

The user friendly code (designated as SEGMENT) can be executed on any UNIX based computer system or on a Apple Macintosh II computer and is available from the Structures and Composites Laboratory at Stanford University.

8. SAMPLE PROBLEMS

Solutions to sample problems were generated to assess the accuracy of the SEGMENT code and to illustrate the type of information provided by the code. The material properties used in the calculations are listed in Table 13.

First we considered a cylindrical segment (arc angle changing between 10° and 180°, inner radius $r^i = 0.1524$ m, thickness $h = 0.508$ mm) made of a $[0/90/+45/-45]_s$ laminate as shown in Fig. 9. The segment is hinged at both straight edges. The outer surface of the segment is subjected to a uniform shear load ($p_\theta^o = 23\,\mathrm{N\,m^{-2}}$).

Table 13. Fiberite T300/934 material data for the sample problems

-Young's moduli
$E_1 = 180.86$ GN/m^2
$E_2 = E_3 = 10.27$ GN/m^2
-Shear moduli
$G_{12} = G_{31} = 7.17$ GN/m^2
$G_{23} = 3.05G$ GN/m^2
-Poisson's ratios
$\nu_{12} = \nu_{31} = 0.28$
$\nu_{23} = 0.49$
-Thermal expansion coefficients
$\alpha_1 = -0.01 * 10^{-6}$/°C
$\alpha_2 = \alpha_3 = 12.5 * 10^{-6}$/°C

The rotation at the hinge, φ, is given by Roark and Young (1986) when the segment is made of an isotropic material and the thickness and width of the segment are small compared to the radius. We calculated a replacement Young's modulus, assuming that a constant bending moment on the thin laminated segment causes the same curvature as on an isotropic arc with the replacement Young's modulus. We found that this modulus is $E_r = 67$ GN m^{-2}.

The rotation at the hinge calculated according to Roark *et al.* is given by a solid line in Fig. 9. The rotation at the hinge was also calculated by the SEGMENT code using the actual material properties given by Table 13. The results of the SEGMENT code are included as open squares in Fig. 9. As can be seen, the results given by Roark and Young and the SEGMENT code agree closely.

Next, we treated the problem of a 90° cylindrical segment (inner radius, $r^i = 3$ mm, thickness $h = 3$ mm) made of 24 plies of unidirectional [0] composite. The segment is subjected to a pure bending of $m_{\theta x} = 11$ Nm m^{-1}. The radial and circumferential stresses in the segment calculated by the SEGMENT code were compared to the stresses given by Girkmann (1956). From Fig. 10, it is seen that the stresses given by the SEGMENT code and Girkmann's formulae agree.

Lastly the stresses and strains and the displacements of an unsupported cylindrical segment were calculated. The inner radius of this segment is $r^i = 0.1524$ m. The lay-up was $[+45/-45/+45/-45]$ (wall thickness $h = 0.508$ mm) and the arc length was 120°. The segment was subjected to uniform temperature change of $\Delta T = 280$°C. The stresses inside

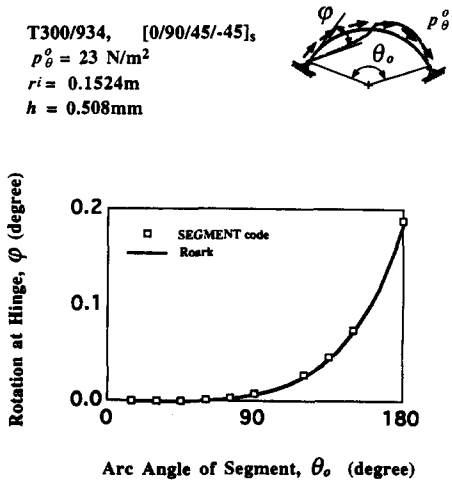

Fig. 9. Angular rotation of a hinged quasi-isotropic $[0/90/45/-45]_s$ segment (inner radius $r^i = 0.1524$ m; thickness $h = 0.508$ mm) under uniform shear load applied on the outer surface $p^o_\theta = 23$ N m^{-2}, as a function of the arc angle θ_o.

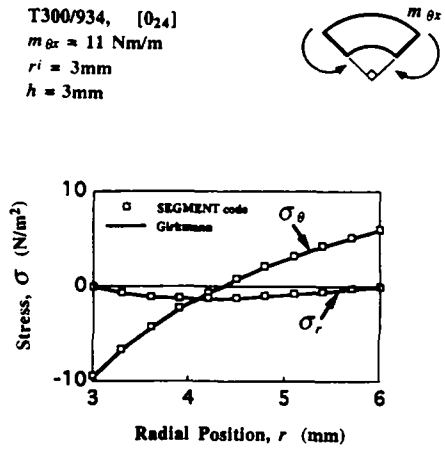

Fig. 10. Circumferential and radial stresses in a unidirectional $[0_{24}]$ thick $\theta_0 = 90^\circ$ segment (inner radius $r^i = 3$ mm; thickness $h = 3$ mm) under pure bending load $m_{0x} = 11$ Nm m^{-1}.

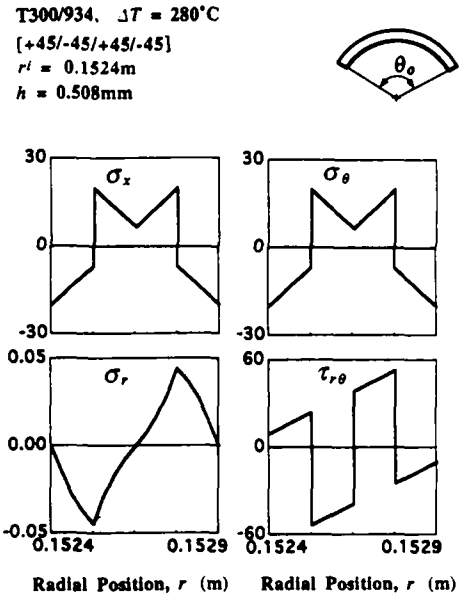

Fig. 11. Stress distribution (N m^{-2}) in a $[45_4/-45_4/45_4/-45_4]$ unsupported $\theta_0 = 120^\circ$ segment (inner radius $r^i = 0.1524$ m; thickness $h = 0.508$ mm) at $\theta = 60^\circ$ subjected to $\Delta T = 280^\circ$C.

the composites calculated by the SEGMENT code are shown in Fig. 11. (The stresses τ_{rx} and $\tau_{x\theta}$ are practically zero, hence are not shown in the figure.) The deformed and undeformed shapes of the segment at two cross-sections ($x = 0$ and $x = 0.1$) are shown in Fig. 12.

9. CONCLUDING REMARKS

The model and the corresponding computer code SEGMENT can be used to calculate the response of composite cylindrical segments subjected to hygrothermal and mechanical loads. Typical computer cpu time of a SUN SPARC station 1 is several minutes. Since the solution requires little time, the code is especially suitable for engineering design.

Acknowledgements—This work was supported in part by the U.S.–Hungarian Joint Fund (J.F. No. 176/91), by ALCOA Laboratories, and by a National Defense Science and Engineering Grant to JMP.

The authors wish to thank Professor George S. Springer for his many constructive comments.

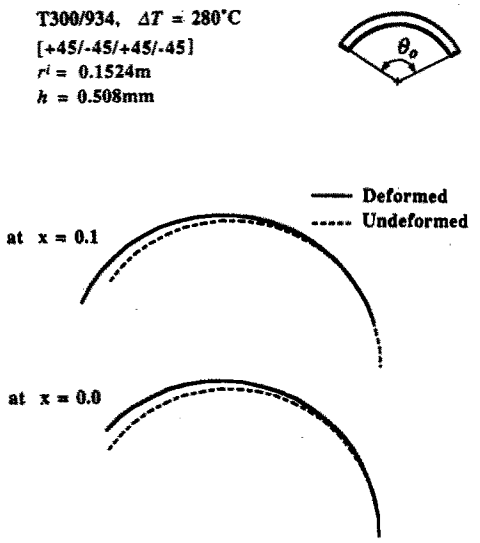

Fig. 12. Displacement (magnified 10 times) of inner radius of a $[45_4/-45_4/45_4-45_4]$ unsupported $\theta_o = 120°$ segment (inner radius $r^i = 0.1524$ m; thickness $h = 0.508$ mm) subjected to $\Delta t = 280°C$.

REFERENCES

Dongarra, J. J., Bunch, J. R., Moler, C. B. and Stewart, G. W. (1978). *LINPACK Users Guide*. SIAM Publications, Philadelphia, PA.

Girkmann, K. (1956). *Flächentragwerke*. Springer, Vienna.

Kollár, L. P., Patterson, J. M. and Springer, G. S. (1992). Composite cylinders subjected to hygrothermal and mechanical loads. *Int. J. Solids Structures* **29**, 1519–1534.

Kollár, L. P. and Springer, G. S. (1992). Stress analysis of anisotropic laminated cylinders and cylindrical segments. *Int. J. Solids Structures* **29**, 1499–1517.

Noor, A. K. and Burton, W. S. (1990). Assessment of computational models for multi-layered composite shells. *Appl. Mech. Rev.* **43**, 67–97.

Noor, A. K., Burton, W. S. and Peters, J. M. (1991). Assessment of computational models for multilayered composite cylinders. *Int. J. Solids Structures* **27**, 1269–1286.

Press, W. H., Flannery, B. P., Teukolsky, S. A. and Vetterling, W. T. (1986). *Numerical Recipes: The Art of Scientific Computing*. Cambridge University Press, Cambridge.

Roark, R. J. and Young, W. C. (1976). *Formulas for Stress and Strain*. McGraw-Hill, London.

Roy, A. K. (1991). Response of thick laminated composite rings to thermal stresses. *Compos. Struct.* **18**, 125–138.

Smith, B. T., Boyle, J. M., Dongarra, J., Garbow, B., Ikebe, Y., Klema, V. C. and Moler, C. B. (1976). *Matrix Eigensystem Routines: EISPACK Guide* (2nd Edn). Springer, New York.

Spencer, A. J. M., Watson, P. and Rogers, T. G. (1991). Mathematical analysis of the springback effect in laminated thermoplastic channel section. *Compos. Manufactur.* **2**, 253–258.

Wolfram, S. (1991). *Mathematica. A System for Doing Mathematics by Computer* (2nd Edn). Addison-Wesley, Redwood City.

APPENDIX A. DISPLACEMENT AND STRESSES

The displacements and stresses proposed by Kollár and Springer (1992) are summarized below. The axial, circumferential and radial displacements in the lth layer have the general form [eqn (1.7)]

$$\begin{aligned} u^l(x,\theta,r) &= u^l_o(x,\theta,r)+u^l_F(\theta,r)+u^l_B(x,\theta,r),\\ v^l(x,\theta,r) &= v^l_o(x,\theta,r)+v^l_F(\theta,r)+v^l_B(x,\theta,r),\\ w^l(x,\theta,r) &= w^l_o(x,\theta,r)+w^l_F(\theta,r)+w^l_B(x,\theta,r). \end{aligned} \tag{A1}$$

In the case of the first two terms on the right-hand side of eqn (A1), denoted by subscripts o and F, the axis of the cylindrical segment remains straight, while in the case of the last term, denoted by subscript B, it is curved. Furthermore, strains calculated from the first term depend on r only; those calculated from the last two terms depend on r and θ.

The functions u^l_o, v^l_o, w^l_o are

$$\begin{aligned} u^l_o &= u^l_a x+u^l_b\theta+u^l_c(r),\\ v^l_o &= v^l_a xr+v^l_b\theta r+v^l_c(r),\\ w^l_o &= w^l_o(r), \end{aligned} \tag{A2}$$

where u_a^l, u_b^l, v_a^l, v_b^l are constants, u_c^l, v_c^l, w_o^l are functions of r, which are given by eqns (1.11), (1.12) and (1.13) and are not reproduced here. These contain six additional constants u_c^l, u_d^l, v_c^l, v_d^l, A_1^l, A_2^l; hence, there are a total number of 10 unknowns in each ply.

Functions u_F^l, v_F^l, w_F^l are

$$u_F^l(\theta,r) = \sum_{j=1} u_j^l(r)\sin j\frac{\pi}{\theta_o}\theta - \sum_{j=1} u_j^{l*}(r)\cos j\frac{\pi}{\theta_o}\theta,$$

$$v_F^l(\theta,r) = \sum_{j=1} v_j^l(r)\sin j\frac{\pi}{\theta_o}\theta - \sum_{j=1} v_j^{l*}(r)\cos j\frac{\pi}{\theta_o}\theta,$$

$$w_F^l(\theta,r) = \sum_{j=1} w_j^l(r)\cos j\frac{\pi}{\theta_o}\theta + \sum_{j=1} w_j^{l*}(r)\sin j\frac{\pi}{\theta_o}\theta, \tag{A3}$$

where $u_j^l(r)$, $v_j^l(r)$, $w_j^l(r)$ are given by eqns (1.44) and are not reproduced here. These contain six unknowns for each Fourier term, denoted by $G_{jk}^l(k = 1,2,\ldots,6)$. Similarly $u_j^{l*}(r)$, $v_j^{l*}(r)$, $w_j^{l*}(r)$ contain six unknowns $G_{jk}^{l*}(k = 1,2,\ldots,6)$.

The displacements u_B^l, v_B^l, w_B^l are

$$\begin{aligned} u_B^l(x,\theta,r) &= u_B^{ly}(x,\theta,r) + u_B^{lz}(x,\theta,r),\\ v_B^l(x,\theta,r) &= v_B^{ly}(x,\theta,r) + v_B^{lz}(x,\theta,r),\\ w_B^l(x,\theta,r) &= w_B^{ly}(x,\theta,r) + w_B^{lz}(x,\theta,r), \end{aligned} \tag{A4}$$

where

$$\begin{aligned} u_B^{ly}(x,\theta,r) &= \kappa^y xr\cos\theta + u_H^{ly}(r)\sin\theta,\\ v_B^{ly}(x,\theta,r) &= \kappa^y\frac{x^2}{2}\sin\theta + v_H^{ly}(r)\sin\theta,\\ w_B^{ly}(x,\theta,r) &= -\kappa^y\frac{x^2}{2}\cos\theta + w_H^{ly}(r)\cos\theta, \end{aligned} \tag{A5}$$

and

$$\begin{aligned} u_B^{lz}(x,\theta,r) &= \kappa^z xr\sin\theta - u_H^{lz}(r)\cos\theta,\\ v_B^{lz}(x,\theta,r) &= -\kappa^z\frac{x^2}{2}\cos\theta - v_H^{lz}(r)\cos\theta,\\ w_B^{lz}(x,\theta,r) &= -\kappa^z\frac{x^2}{2}\sin\theta + w_H^{lz}(r)\sin\theta. \end{aligned} \tag{A6}$$

In these expressions y refers to the case when the axis is curved in the x–y plane; z refers to the case when the axis is curved in the x–z plane. κ^y and κ^z are the curvatures in the x–y and x–z planes.

$u_H^{ly}(r)$, $v_H^{ly}(r)$, $w_H^{ly}(r)$ are given by eqns (1.54). They contain six unknowns denoted by $H_k^{ly}(k = 1,2,\ldots,6)$. Similarly $u_H^{lz}(r)$, $v_H^{lz}(r)$, $w_H^{lz}(r)$ contain six unknowns $H_k^{lz}(k = 1,2,\ldots,6)$.

The unknowns are listed in Table 1.

In Table A1 we list the displacement terms and the stresses. For u_o, v_o, w_o, the stresses depend on r only. In the other stress expressions, the terms denoted by $\hat{}$ depend on r only.

Table A1. The displacement, temperature and stress terms

	u_o, v_o, w_o	u_F, v_F, w_F		u_B, v_B, w_B	
u		$u_j(r)\sin j\frac{\pi}{\theta_o}\theta$	$-u_j^*(r)\cos j\frac{\pi}{\theta_o}\theta$	u_B^y, v_B^y, w_B^y	u_B^z, v_B^z, w_B^z
v		$v_j(r)\sin j\frac{\pi}{\theta_o}\theta$	$-v_j^*(r)\cos j\frac{\pi}{\theta_o}\theta$		
w		$w_j(r)\cos j\frac{\pi}{\theta_o}\theta$	$w_j^*(r)\sin j\frac{\pi}{\theta_o}\theta$		
ΔT	$\sum_{i=0}\Delta T_{oi}(r)^i$	$\left[\sum_{i=0}\Delta T_{ji}(r)^i\right]\cos j\frac{\pi}{\theta_o}\theta$	$\left[\sum_{i=0}\Delta T_{ji}(r)^i\right]\sin j\frac{\pi}{\theta_o}\theta$		
σ_z	σ_{zo}	$\sigma_{zj} = \hat{\sigma}_{zj}\cos j\frac{\pi}{\theta_o}\theta$	$\sigma_{zj}^* = \hat{\sigma}_{zj}^*\sin j\frac{\pi}{\theta_o}\theta$	$\sigma_{zB}^y = \hat{\sigma}_{zB}^y\cos\theta$	$\sigma_{zB}^z = \hat{\sigma}_{zB}^z\sin\theta$
σ_θ	$\sigma_{\theta o}$	$\sigma_{\theta j} = \hat{\sigma}_{\theta j}\cos j\frac{\pi}{\theta_o}\theta$	$\sigma_{\theta j}^* = \hat{\sigma}_{\theta j}^*\sin j\frac{\pi}{\theta_o}\theta$	$\sigma_{\theta B}^y = \hat{\sigma}_{\theta B}^y\cos\theta$	$\sigma_{\theta B}^z = \hat{\sigma}_{\theta B}^z\sin\theta$
σ_r	σ_{ro}	$\sigma_{rj} = \hat{\sigma}_{rj}\cos j\frac{\pi}{\theta_o}\theta$	$\sigma_{rj}^* = \hat{\sigma}_{rj}^*\sin j\frac{\pi}{\theta_o}\theta$	$\sigma_{rB}^y = \hat{\sigma}_{rB}^y\cos\theta$	$\sigma_{rB}^z = \hat{\sigma}_{rB}^z\sin\theta$
$\tau_{\theta r}$	$\tau_{\theta ro}$	$\tau_{\theta rj} = \hat{\tau}_{\theta rj}\sin j\frac{\pi}{\theta_o}\theta$	$\tau_{\theta rj}^* = \hat{\tau}_{\theta rj}^*\cos j\frac{\pi}{\theta_o}\theta$	$\tau_{\theta rB}^y = \hat{\tau}_{\theta rB}^y\sin\theta$	$\tau_{\theta rB}^z = \hat{\tau}_{\theta rB}^z\cos\theta$
τ_{rz}	τ_{rzo}	$\tau_{rzj} = \hat{\tau}_{rzj}\sin j\frac{\pi}{\theta_o}\theta$	$\tau_{rzj}^* = \hat{\tau}_{rzj}^*\cos j\frac{\pi}{\theta_o}\theta$	$\tau_{rzB}^y = \hat{\tau}_{rzB}^y\sin\theta$	$\tau_{rzB}^z = \hat{\tau}_{rzB}^z\cos\theta$
$\tau_{z\theta}$	$\tau_{z\theta o}$	$\tau_{z\theta j} = \hat{\tau}_{z\theta j}\cos j\frac{\pi}{\theta_o}\theta$	$\tau_{z\theta j}^* = \hat{\tau}_{z\theta j}^*\sin j\frac{\pi}{\theta_o}\theta$	$\tau_{z\theta B}^y = \hat{\tau}_{z\theta B}^y\cos\theta$	$\tau_{z\theta B}^z = \hat{\tau}_{z\theta B}^z\sin\theta$

APPENDIX B. SURFACE LOADS

Let the displacements be given by eqns (A1)–(A3), provided that $u_B^l = v_B^l = w_B^l = 0$. The stresses due to these displacements form a Fourier series (Table A1). Hence, we have to express the loads in terms of a Fourier series as well. Let the load be

$$p_x^{i,o} = \sum_{j=0} \hat{p}_{xj}^{i,o} \sin j\frac{\pi}{\theta_o}\theta + \sum_{j=0} \hat{p}_{xj}^{i,o*} \cos j\frac{\pi}{\theta_o}\theta,$$

$$p_\theta^{i,o} = \sum_{j=0} \hat{p}_{\theta j}^{i,o} \sin j\frac{\pi}{\theta_o}\theta + \sum_{j=0} \hat{p}_{\theta j}^{i,o*} \cos j\frac{\pi}{\theta_o}\theta,$$

$$p_r^{i,o} = \sum_{j=0} \hat{p}_{rj}^{i,o} \cos j\frac{\pi}{\theta_o}\theta + \sum_{j=0} \hat{p}_{rj}^{i,o*} \sin j\frac{\pi}{\theta_o}\theta, \tag{B1}$$

where $\hat{p}$ and $\hat{p}^*$ are constants. These equations apply at both the inner (superscript i) and outer (superscript o) surfaces. Substituting these surface loads and the stresses given by Table A1 into eqns (16) and (17), we obtain the set of equations given in Table B1.

However, the surface loads together with the boundary forces have to be in equilibrium. The investigation of the equilibrium equations shows that some of the surface loads cannot be specified independently [see Kollár *et al.* (1992)]. It can be shown that for $j = 0$ only four (instead of six), and for the special case when $j(\pi/\theta_o) = 1$ only 10 (of the 12) surface loads are independent. Thus, two of the boundary conditions for $j = 0$, and $j(\pi/\theta_o) = 1$ cannot be used. These are indicated by the brackets in Table B1.

Note, that this reduction on the boundary conditions is in agreement with the required ones (see Table 1).

Table B1. Stress boundary conditions

For j=0

$$\begin{aligned} \hat{p}_{ro}^{i} &= \sigma_{ro}^{1} \\ \hat{p}_{\theta o}^{i*} &= \sigma_{r\theta o}^{1} \qquad \text{at } r=r^{i} \\ \hat{p}_{xo}^{i*} &= \tau_{rxo}^{1} \end{aligned} \tag{B2}$$

$$\begin{aligned} \hat{p}_{ro}^{o} &= \sigma_{ro}^{n} \\ (\hat{p}_{\theta o}^{o*} &= \sigma_{r\theta o}^{n}) \qquad \text{at } r=r^{o} \\ (\hat{p}_{xo}^{o*} &= \tau_{rxo}^{n}) \end{aligned} \tag{B3}$$

For $j\frac{\pi}{\theta_o} = 1$

$$\begin{aligned} \hat{p}_{rj}^{i} &= \hat{\sigma}_{rj}^{1} \quad \hat{p}_{rj}^{i*} = \hat{\sigma}_{rj}^{1*} \\ \hat{p}_{\theta j}^{i} &= \hat{\sigma}_{r\theta j}^{1} \quad \hat{p}_{\theta j}^{i*} = \hat{\sigma}_{r\theta j}^{1*} \qquad \text{at } r=r^{i} \\ \hat{p}_{xj}^{i} &= \hat{\tau}_{rxj}^{1} \quad \hat{p}_{xj}^{i*} = \hat{\tau}_{rxj}^{1*} \end{aligned} \tag{B4}$$

$$\begin{aligned} \hat{p}_{rj}^{o} &= \hat{\sigma}_{rj}^{n} \quad \hat{p}_{rj}^{o*} = \hat{\sigma}_{rj}^{n*} \\ (\hat{p}_{\theta j}^{o} &= \hat{\sigma}_{r\theta j}^{n}) \quad (\hat{p}_{\theta j}^{o*} = \hat{\sigma}_{r\theta j}^{n*}) \qquad \text{at } r=r^{o} \\ \hat{p}_{xj}^{o} &= \hat{\tau}_{rxj}^{n} \quad \hat{p}_{xj}^{o*} = \hat{\tau}_{rxj}^{n*} \end{aligned} \tag{B5}$$

For $j\frac{\pi}{\theta_o} \neq 1$

$$\begin{aligned} \hat{p}_{rj}^{i} &= \hat{\sigma}_{rj}^{1} \quad \hat{p}_{rj}^{i*} = \hat{\sigma}_{rj}^{1*} \\ \hat{p}_{\theta j}^{i} &= \hat{\sigma}_{r\theta j}^{1} \quad \hat{p}_{\theta j}^{i*} = \hat{\sigma}_{r\theta j}^{1*} \qquad \text{at } r=r^{i} \\ \hat{p}_{xj}^{i} &= \hat{\tau}_{rxj}^{1} \quad \hat{p}_{xj}^{i*} = \hat{\tau}_{rxj}^{1*} \end{aligned} \tag{B6}$$

$$\begin{aligned} \hat{p}_{rj}^{o} &= \hat{\sigma}_{rj}^{n} \quad \hat{p}_{rj}^{o*} = \hat{\sigma}_{rj}^{n*} \\ \hat{p}_{\theta j}^{o} &= \hat{\sigma}_{r\theta j}^{n} \quad \hat{p}_{\theta j}^{o*} = \hat{\sigma}_{r\theta j}^{n*} \qquad \text{at } r=r^{o} \\ \hat{p}_{xj}^{o} &= \hat{\tau}_{rxj}^{n} \quad \hat{p}_{xj}^{o*} = \hat{\tau}_{rxj}^{n*} \end{aligned} \tag{B7}$$